

CIPS RAA Level 2 Data: Orbit-by-Orbit Rayleigh Albedo Anomaly

Last updated July 2020

1. Introduction

This document describes the CIPS Level 2 Rayleigh albedo anomaly (RAA) data (Randall *et al.*, 2017). Briefly, CIPS measures the single-scatter albedo at 265 nm, which in the absence of polar mesospheric clouds (PMCs) is due entirely to atmospheric Rayleigh scattering. The source function of the observed Rayleigh scattering peaks near an altitude of 50–55 km (Bailey *et al.*, 2009). The Rayleigh scattering albedo at 265 nm is controlled by the atmospheric neutral density and is modulated strongly by ozone absorption (McPeters, 1980). Coherent perturbations to the observed Rayleigh scattering signal on scales of tens to hundreds of kilometers are generally indicative of variations in the neutral density and/or ozone near 50–55 km induced by gravity waves (GWs). To quantify these variations, the RAA is defined as the residual difference between the observed Rayleigh scattering albedo and a baseline albedo that would be observed in the absence of any small-scale atmospheric variations, expressed in %. The RAA signal therefore provides a direct measure of dynamical perturbations near the stratopause. In particular, the occurrence and spatial characteristics of GWs with typical horizontal wavelengths from about 15-600 km and vertical wavelengths longer than 15 km can be derived from the measured RAA.

2. CIPS Observing Modes and Data Availability

The RAA data product is derived using all available dayside CIPS images throughout the year. From 24 May 2007 through 11 February 2016 CIPS operated in the “summer pole” imaging mode. In this mode, overlapping, four-camera images (“scenes”; see Figure 1) were obtained every 43 seconds at northern hemisphere (NH) latitudes of about 40°N-85°N from March equinox to September equinox, and at southern hemisphere (SH) latitudes of about 40°S-85°S from September equinox to March equinox.

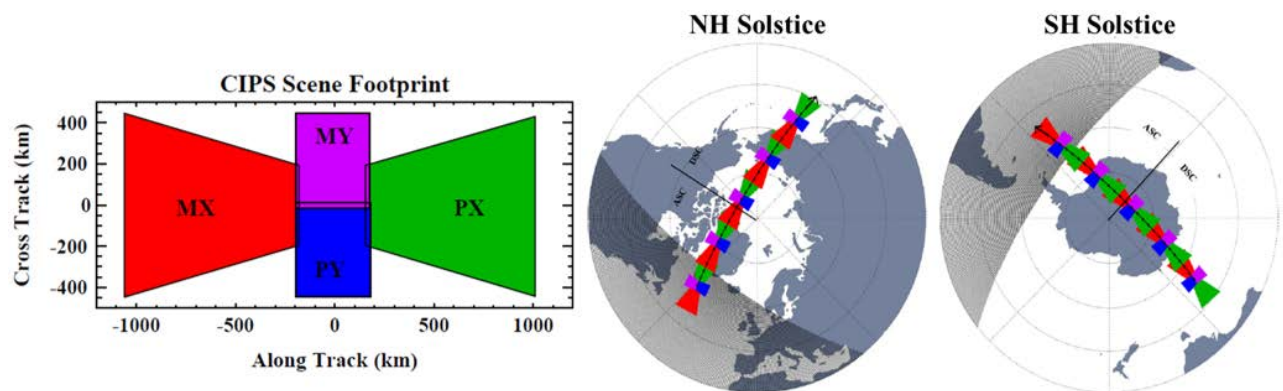


Figure 1. This diagram illustrates the relative alignment of the four CIPS cameras and “summer pole” sampling for an example orbit. The two “X” cameras point in the forward and aft direction, while the “Y” cameras have a primarily nadir orientation. The distance scales indicate the geometric footprint of a CIPS scene at the nominal PMC cloud deck altitude of 83 km. The PX camera always points in the sunward direction, which corresponds to the satellite ram (anti-ram) for Northern (Southern) Hemisphere measurements. The sampling along the orbit pertained to satellite operations from launch until 11 February 2016. The same camera colors are used in later figures. Adapted from Lumpe *et al.* (2013).

Full coverage of the sunlit hemisphere became possible starting in March 2016 when the CIPS instrument began operating in “continuous imaging” (CI) mode. In CI mode from March of 2016 until early November of 2018, images were taken on a 3-minute cadence over the entire orbit. Figure 2 shows an example of this full-orbit CI mode sampling, with pole-centered views for the NH (left) and SH (right). Since the images were acquired throughout the orbit, they included the eclipsed (night side) of the earth; however, images taken on the night side are not valid for scientific analysis. During the full-orbit CI time period the beta angle (i.e., the angle between the orbital plane of the satellite and the vector to the Sun) changed significantly. From 24 February 2017 until 23 November 2017 the satellite was in “full-sun” conditions, without eclipses. Unfortunately, roll control issues during this period of time prevented the acquisition of reliable calibration data, so no CIPS data are available. From 7-25 Feb 2018 CIPS was off in preparation for entering the second full-sun period. For this full-sun period, the sampling during which is illustrated in Figure 3, the satellite remained nadir-pointed. Full-sun CIPS data are thus available from 26 February until 20 September 2018. CIPS was off to prepare to exit full-sun conditions from 21-28 September 2018, at which point the sampling was similar to that depicted in Figure 2.

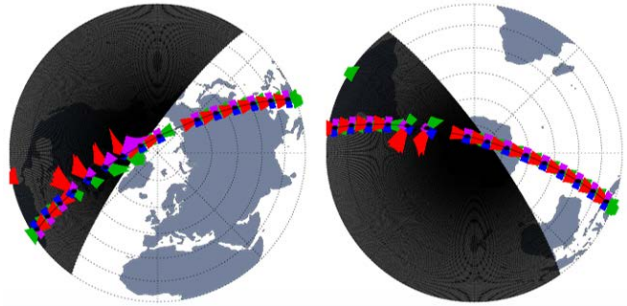


Figure 2. Example of CIPS sampling for full-orbit Continuous Imaging including eclipses. Pole-centered views are shown for the NH (left) and SH (right); black shading indicates the night side. For illustration only; the exact geometry varies from orbit-to-orbit and day-to-day.

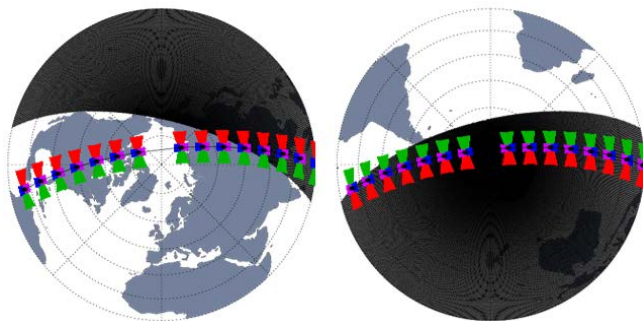


Figure 3. As in Figure 2, but for “full-sun” conditions, when CIPS images were near the terminator.

On 3 November 2018 CIPS was commanded to take all of its images over a period of ~70 minutes in order to confine imaging to sunlit latitudes. An example of this sampling is shown in Figure 4. The image acquisition time was modified to 60 minutes in October of 2019 when the eclipse duration lengthened.

Table 1 summarizes the time periods of CIPS RAA data availability. As of July 2020, RAA data are available during most months since the launch of AIM in 2007. The longest periods without data are the time periods from (1) March of 2008 through March of 2010, (2) early August to mid October of 2016, and (3) late February to late November of 2017. During those time periods the instrument was either off or RAA retrievals were complicated by spacecraft operations.

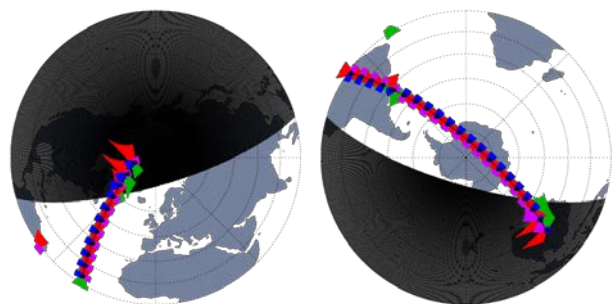


Figure 4. As in Figure 2, but for CI mode confined to the sunlit side of the orbit.

Expectations are that the retrievals can be corrected for the 2008-2010 time period, but data from time periods (2) and (3) are unlikely to be recovered.

Table 1. CIPS RAA Data Availability

Dates (yyyymmdd)	Notes
20070524-20080207	Summer pole imaging
20080208-20080320	Unavailable. CIPS was off after safing on 8 February.
20080321-20100403	Unavailable. Roll issues complicate retrievals; probably recoverable.
20100404-20160211	Summer pole imaging
20160212-20160228	Unavailable. Transition to Continuous Imaging.
20160301-20160805	Continuous Imaging (CI) including eclipses, but no night-side retrievals.
20160806-20161014	Unavailable. Various satellite operational anomalies.
20161015-20170223	Continuous Imaging (CI) including eclipses, but no night-side retrievals.
20170224-20171123	Unavailable. Transition to 1 st full-sun period, unreliable calibration data while in full-sun, and exit out of full-sun; unlikely to recover.
20171124-20180206	CI including eclipses, but no night-side retrievals.
20180207-20180225	Unavailable. Transition to 2 nd full-sun period.
20180226-20180920	CI in full-sun.
20180921-20180928	Unavailable. Exit out of full-sun.
20180929-20181102	CI including eclipses, but no night-side retrievals.
20181103-Present	CI dayside only

3. RAA Data Products

The RAA processing stream starts with the same Level 1A data used for PMC data processing (*Lumpe et al., 2013*) and produces Level 2 RAA files for both scene-by-scene (level 2A) and full orbit strip (level 2B) data, as described in detail below. As of July 2020, the Level 1A data are version 5.20, revision 01, and level 2 RAA data are version 1.10 revision 05. Validation of the RAA data is ongoing, but *Randall et al. (2017)* presented several case studies that compare CIPS GW retrievals to near-coincident observations by the Atmospheric Infrared Sounder (AIRS) instrument. These comparisons show good agreement in the location, orientation and horizontal wavelengths of GW features in both the CIPS and AIRS imagery. The brightness temperature weighting function for the 4.3 μm AIRS data peaks around 35 km, whereas the CIPS weighting function peaks around 50-55 km, enabling investigation of upward propagating GWs.

The RAA data product is provided in two different formats for scientific analysis. Level 2A files contain CIPS RAA data in a scene-by-scene format. A CIPS scene contains simultaneous images from the four CIPS cameras, with a footprint of approximately 2000 km by 900 km (*Lumpe et al., 2013*). The orientation of the scenes with respect to the orbit track has varied over the course of the mission, as shown in Figures 1-4. In the Level 2B files all scenes from an orbit are merged together by combining overlapping pixels from different cameras in much the same way as the CIPS Level 2 PMC data products (again, see *Lumpe et al., 2013*). For both levels 2A and 2B, data files are produced on an orbit-by-orbit basis. The following files are made publicly available for each orbit:

Level 2A

- Geolocation NetCDF file, including variables such as date, time, latitude, longitude, solar zenith angle, etc. The file name is *cat.nc (“cat” is short for “catalog”).
- Rayleigh Albedo Anomaly NetCDF file, including derived RAA and RAA error, and diagnostics. The file name is *alb.nc.
- Measurement geometry NetCDF file, containing satellite view angles and scattering angles for each scene. The file name is *ang.nc.

Level 2B

- Geolocation NetCDF file, including variables such as date, time, latitude, longitude, solar zenith angle, etc. File content is similar to the Level 2A cat file. The file name is *cat.nc.
- Rayleigh Albedo Anomaly NetCDF file, including derived RAA and RAA error, and total measured Rayleigh albedo. The file name is *alb.nc.
- Orbit strip png image of RAA. The file name is *alb.png.

Variables contained in all NetCDF files are described in tables at the end of this document. There are ~15 orbits per day. In summer pole imaging mode, each orbit contains 30 PX camera images and 27 images from each of the other three cameras (i.e., 27 four-camera scenes plus 3 extra PX images), while in CI mode there are typically 30 images per camera (i.e., 30 four-camera scenes). Level 2 RAA and associated geolocation variables are provided with a horizontal resolution of 56.25 km² over the entire orbit track. Resolution elements are 7.5 km × 7.5 km in the nadir and become elongated away from nadir, but remain 56.25 km² in total area covered.

Data arrays in the Level 2 files are reported for all Level 2 pixels, with array dimensions corresponding to the number of elements in the along-track and cross-track directions. For convenience in data handling, the arrays span the entire bounding box defined by a single CIPS scene (Level 2A) or the entire orbit (Level 2B). However roughly half of these elements correspond to locations where no measurements are made and therefore have fill values. The compressed Level 2A geolocation, albedo and measurement geometry NetCDF files are ~11, 6.3, and 18 MB in size, respectively. Compressed Level 2B geolocation and albedo NetCDF files are ~22 and 4.1 MB in size, respectively. Uncompressed file sizes are much larger due to the significant fraction of fill (NaN) values in these files. IDL software tools to read the Level 2 RAA netcdf files are available for download from the CU-LASP and NASA SPDF web sites. NetCDF readers for other software packages are available elsewhere (e.g., <http://www.unidata.ucar.edu/software/netcdf/software.html>).

Users interested in conducting a precise, quantitative analysis of GW wavelengths and amplitudes are encouraged to use the level 2A data product. Users interested in a more qualitative view of the data are encouraged to use the Level 2B data product. The advantage of using the level 2B data is that these provide the context of an entire orbit, and waves are often visible in multiple scenes. The disadvantage for quantitative analyses is that, for most of the AIM data set, the scenes overlap one another, so wave characteristics in the overlap regions can be obscured in the level 2B data.

4. Orbit Strip Images

For a quick, qualitative overview of the CIPS data, users are encouraged to peruse the level 2B png files, which contain images of the orbit strips. These images often show visual evidence of GW features that can then be analyzed more carefully using the data in the NetCDF files. Figure 5 shows a few examples of the level 2B orbit strips. These examples are representative of orbit strips that contain clear signatures of GWs, and were chosen to illustrate how the CIPS sampling and scene orientation has changed over time. Gaps in the image sequences, such as shown in Figures 5b and 5d, correspond to the locations of dark images, which are required for calibration, or yaw maneuvers, which occur twice per orbit.

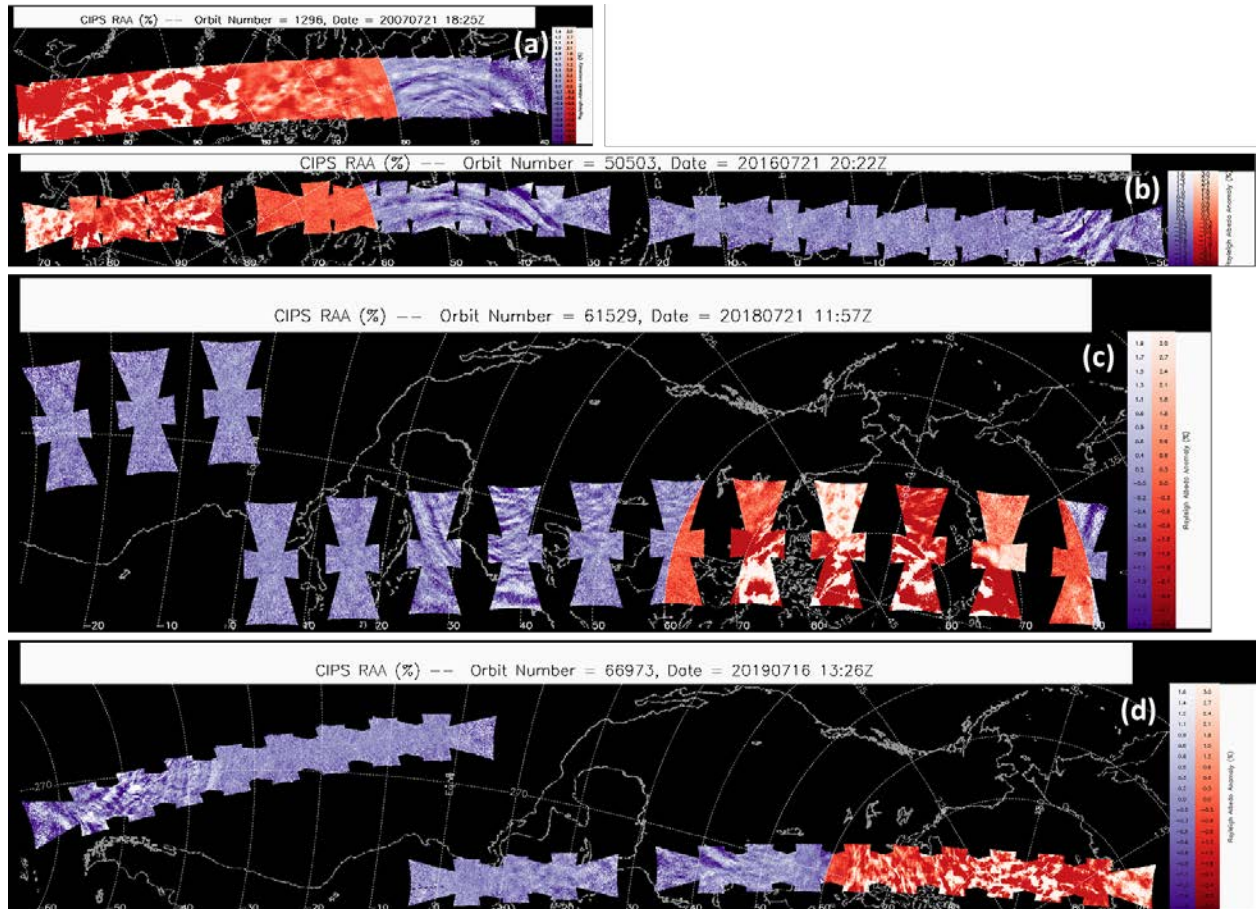


Figure 5. Example RAA level 2B orbit strips from July in 2007, 2016, 2018, and 2019 (top to bottom). Corresponding observing modes are (a) summer pole, (b) CI including eclipses, (c) CI in full-sun, (d) CI dayside only. Red/orange shading indicates the approximate PMC region, within which structure is more likely due to PMCs near 83 km than to GWs near 50-55 km.

The data shown in Figure 5 were all acquired during the NH PMC season. PMCs alter the observed albedo, and these effects cannot be removed from the RAA data product. Therefore, the region where PMCs are most often observed, from 60° to the pole, is shaded red/orange in the png files. Users should be cautious when using data in the red/orange shaded region, since the observed structure is likely, although not necessarily, caused by PMCs, not GWs. Users should also be aware that PMCs can occur at lower latitudes where the png plots are colored in shades of purple (see discussion of Figure 9 below).

5. Cautions to Users

This section describes some anomalies or artifacts in the RAA data of which users should be aware. Some of these are simply results of the observing geometry, but others are caused by retrieval artifacts or PMC contamination. If images are found to exhibit suspicious behavior that is not described here, please inform us by sending an email to aimstds@lasp.colorado.edu. The CIPS team is developing a data product that quantifies the wave variance, which when available (anticipated in late 2020) will facilitate automated analysis of the RAA data. A brief description of the variance data product is described below.

PX Camera Edge and Corner Artifacts in 2007-2008

For reasons that are being investigated as of July 2020, much of the RAA data in 2007-2008 exhibit high-RAA artifacts in the corners or edges of the PX camera. Figure 6 shows an example of this for orbit 1451, on 1 August 2007. Early indications are that these signals are small enough that they will not lead to significant values of the wave variance, but at the time of this writing, caution is warranted when interpreting such data. More generally, if repeating patterns occur in multiple adjacent scenes, caution is warranted.

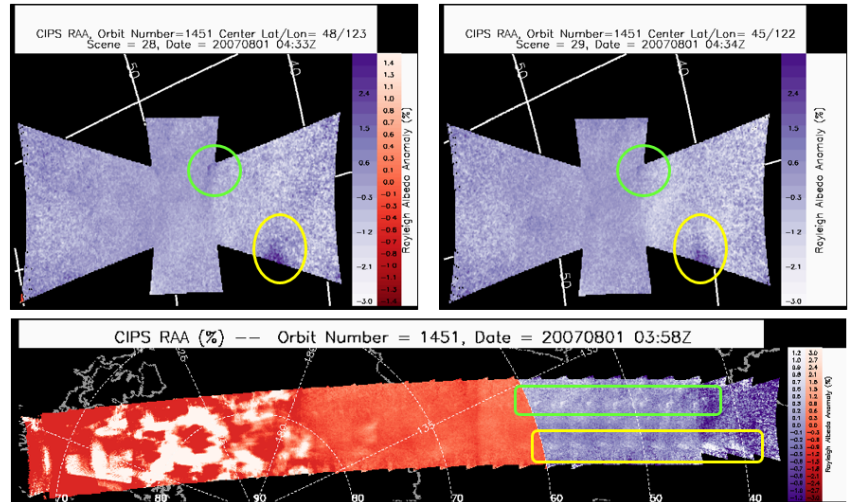


Figure 6. Plots of Level 2A (top) and 2B (bottom) RAA data for orbit 1451 on 1 August 2007. The level 2A scenes shown are for scene 28 (left) and 29 (right), which are the two right-most scenes in the level 2B orbit strip. Artifacts mentioned in the text are highlighted in yellow (edge) or green (corner). Note that the level 2A images are plotted with a color scale that goes from light at the low end to dark at the high end, the opposite of the level 2B color scale. The level 2A png plots are being reprocessed in July 2020 to reverse the color scale.

Discontinuities at Camera Edge/Corner Overlap Regions

Users will note that in some level 2B data, discontinuities appear in regions where a nadir or near-nadir edge of one camera overlaps with a corner of the fore or aft camera. An example of this is shown in Figure 7, for orbit 48633 on 20 March 2016. These discontinuities reflect the fact that camera pixels in the fore and aft regions are elongated relative to nadir pixels. The science data is binned into pixels that all have a uniform area of 56 km², so this means that more native pixels (4 km²) are combined into each science pixel in the nadir than in the fore and aft regions of the scenes. The result is that there is often larger uncertainty in the fore and aft regions than in the nadir or near-nadir regions. Figure 7 shows part of the level 2B png image for orbit 48633, with several of the discontinuities highlighted by the green boxes. Figure 7 also shows the RAA uncertainty for the entire orbit, with the same regions highlighted with black boxes. The uncertainty is plotted with a

different projection than the RAA itself, but clearly shows the higher uncertainty in the corners of the fore and aft cameras. The discontinuities in the level 2B png images occur at the boundary between regions where pixels in one camera are closer to nadir than the pixels in the overlapping camera. The pixels closer to nadir have lower uncertainties, whereas the fore or aft pixels have higher uncertainties.

Orbit Strip Edge Scenes

In addition to the aforementioned discontinuities in the edge/corner overlap regions, individual cameras in the scenes on the edges of orbit strips often have RAA values that are either systematically higher or systematically lower than scenes in the rest of the orbit. Figure 8 gives an example of this. The top panel shows the full level 2B RAA orbit strip for orbit 72288 on 1 July 2020. Except for very small corner regions, the left-hand camera on the southernmost scene is uniformly darker purple (lower RAA) than the rest of the scene or than other scenes. The level 2A png plot for this single scene is shown on the bottom left (note that it is plotted with a color scale that ranges from -3 to +3 instead of from -1.6 to +1.6, and that the colors are reversed, with white indicating more negative values). The RAA uncertainty for this scene is shown in the bottom right, plotted with a slightly different projection.

For comparison, the RAA itself is plotted in the middle panel with the same projection as the uncertainty. It is clear that the uniformly more negative RAA values in the leftmost camera are associated with higher values of uncertainty. At the current time, the cause(s) of this type of artifact is (are) not understood. The fundamental issue is an error in subtracting the background Rayleigh scattering albedo from the observed albedo for scenes that are on the edges of orbit strips. Since this error is a systematic retrieval error, it is not represented in the uncertainty values. As in the example of Figure 7, the high uncertainties do reflect the reduced signal-to-noise that arises from the elongated native pixels in the fore and aft cameras. In addition, the higher solar zenith angles associated with this scene means lower radiances, further reducing the signal-to-noise. The CIPS team is working to develop a procedure that will enable users to screen these scenes.

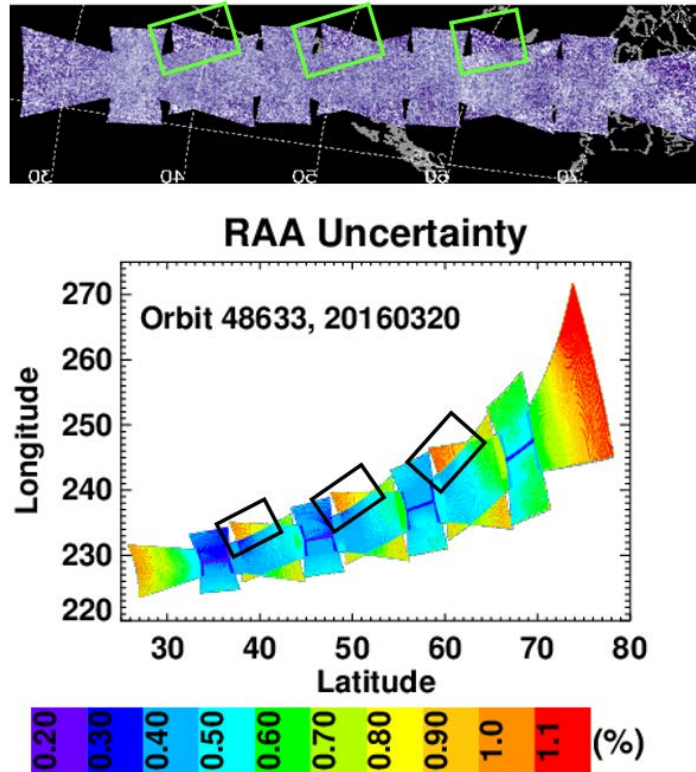


Figure 7. Level 2B RAA for orbit 48633 on 20160320 (top) and corresponding uncertainty (bottom), plotted with a different projection. Corners of the fore and aft cameras (PX and PY) are associated with higher uncertainties because fewer native pixels are binned in the 56 km² science pixels. The different native pixel resolutions can result in discontinuities such as highlighted in the boxes. Users should consider uncertainties when analyzing the data.

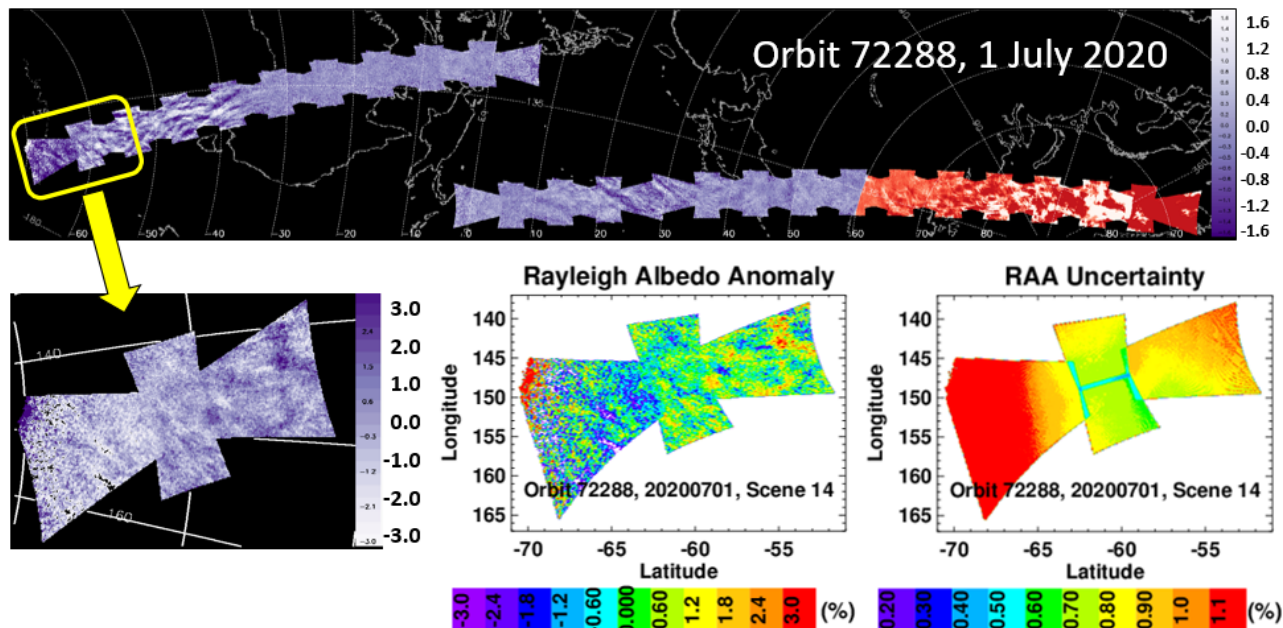


Figure 8. Top: Level 2B RAA for orbit 72288 on 20200701. Bottom Left: RAA from the southern-most scene (14) from orbit 72288, from the level 2A CIPS png file. Note the reversed color scale, with a different range from the level 2B data in the top panel. The RAA is replotted in the bottom middle panel with a different color table and slightly different projection, which matches the plot of the RAA uncertainty on the bottom right. Note the relatively high uncertainty in the left edge camera (i.e., red region), which is associated with the overall more negative RAA in this camera (i.e., dark purple in the level 2B data). Caution is warranted when interpreting edge scenes because of the generally higher uncertainties associated with these scenes. The missing upper left corner of the scene corresponds to solar zenith angles greater than 94 degrees, which are not included in the retrievals because of the low light levels.

Signatures of PMCs in the RAA Data

The RAA retrieval is registered to an altitude near 53 km, so it cannot be used for quantitative analyses of PMCs. However, because PMCs modify the amount of 265-nm radiation scattered by the atmosphere, signatures of PMCs are apparent in the RAA data. These signatures can be seen in many of the examples shown above, in the red/orange shaded region of the RAA plots. Although PMCs most often occur poleward of 60° latitude in each hemisphere, they have been observed at latitudes as low as 35°. Therefore, signatures of PMCs can sometimes be found in the RAA data equatorward of 60°. Figure 9 shows an example of a relatively low latitude PMC detection in the RAA data. PMC signatures are generally much more chaotic than GW signatures, and they are also often easy to identify because they appear as extensions of patterns that are apparent in the red/orange shaded region. Finally, PMCs would typically only appear equatorward of 60° in the CIPS data near the peak of the PMC season, in late June to early July in the NH and in late December to early January in the SH.

An interesting aspect of this discussion is that, unlike the PMC retrievals, the RAA retrievals have no filtering to avoid false detections of PMCs. The PMC retrieval filtering effectively avoids false detections, but in so doing fails to identify some of the dimmest PMCs. Therefore, more PMC signatures are often evident in the RAA data than in the PMC data. This is why the PMC albedo,

which is shown in Figure 9 for the same orbit as the RAA data, does not show the lowest latitude clouds that are evident in the RAA data.

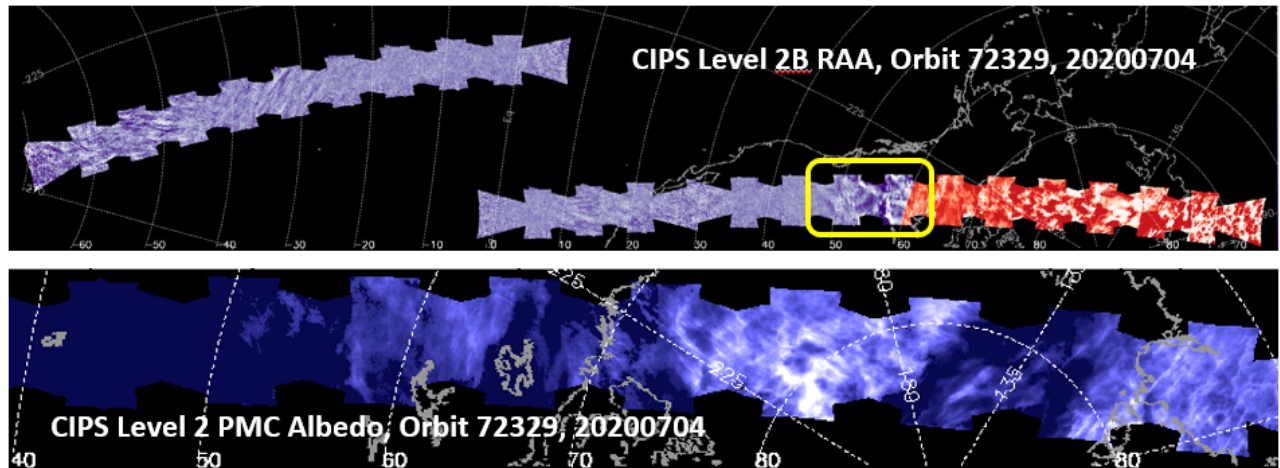


Figure 9. Top: Example of PMC signatures in the level 2B RAA data from 4 July 2020, orbit 72329. Bottom: PMC albedo for the same orbit. The RAA data show evidence for many more clouds from 50-60°N, because no screen is applied to avoid false cloud detections. Although the RAA data cannot be used for quantitative analyses of PMCs, it can be used to identify dim PMCs that the operational PMC algorithm misses.

RAA Wave Variance

Users are encouraged to consider the RAA uncertainties, which are provided with both the level 2A and 2B data, when analyzing the data. In addition, the CIPS team is developing a new RAA wave variance data product to facilitate automated analyses of the RAA data. The goal here is to develop a product that distinguishes between RAA variations due to waves and variations caused by artifacts. The RAA variance is derived from the level 2A RAA data. Each level 2A scene is converted to wavenumber space using a fast Fourier transform. Ninth order Butterworth filters are used to create a window filter designed to remove structure with horizontal wavelength less than 22.5 km (~ 3 pixels) and greater than 600 km. The data are then converted back to the original domain, with pixels matching the RAA level 2A scenes. To further reduce noise, a 5x5 pixel smoothing is applied wherever the systematic RAA uncertainty, which increases toward the edge of the camera field of view, is greater than 0.65%; a 3x3 pixel smoothing is applied when the uncertainty is less than 0.65%. Variance of the filtered RAA is determined at every pixel for the surrounding 11x11 pixel neighborhood, or 6800 km². Due to large edge effects in pre-continuous-imaging seasons, solar zenith angles less than 44° are not considered for orbits prior to March of 2016. For all orbits, pixels with solar zenith angle greater than 85° are omitted.

Figure 10 shows an example of the RAA for orbit 50503 (as in Figure 5b) and the associated wave variance. The wave variance is plotted with two color scales. The black/gray colored region denotes the PMC region, which should not be analyzed for wave activity when PMCs are clearly present. The peach/orange colored region (with the lowest contour level colored light yellow) shows the wave variance outside the PMC region. This data product is still being evaluated, but initial indications are that values of the variance greater than $\sim 0.1\%^2$ indicate waves. This value is indicated by the first black contour in the peach region of the variance plot. In Figure 10, it is clear that the gravity waves evident in the RAA plot are associated with variances greater than $0.1\%^2$, and other regions without obvious waves are associated with lower variances. In particular, upon

close inspection it is clear that, like the example in Figure 7, this orbit does show discontinuities when the near-nadir edge of one camera overlaps the corner of another. The wave variances for these regions are insignificant, however, so these discontinuities would not be identified as waves.

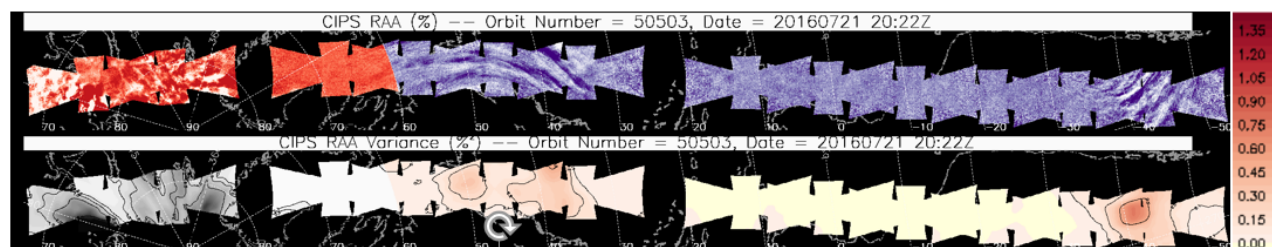


Figure 10. CIPS RAA (top) and RAA wave variance (bottom) for orbit 50503 on 20160721. Preliminary evaluations suggest that RAA variations due to actual waves can be identified reliably as having wave variances of $0.1\%^2$ or greater, whereas variations due to noise or retrieval artifacts have smaller variances. The PMC region is denoted in orange/red shading in the top panel, and black/gray shading in the bottom panel, and is not recommended for wave analyses.

Figure 11 shows the RAA and RAA wave variance for orbit 1451 on 20070801. As discussed above (see Figure 6), this orbit exhibits artifacts that are often present in the data from 2007-2008, but that are not yet understood. Although these artifacts appear quite obvious to the eye, as shown in the bottom panel of Figure 11, they are not associated with significant wave variances.

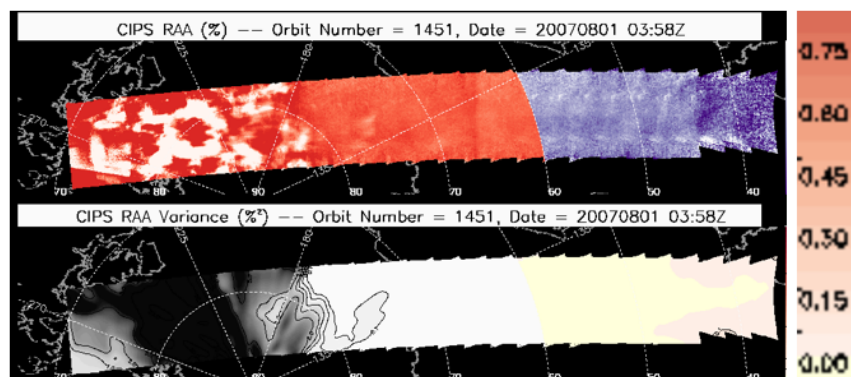


Figure 11. As in Figure 10, but for orbit 1451 on 20070801.

6. NetCDF Files

The NetCDF files listed in Section 3 enable users to quantitatively analyze the data plotted in the orbit strip images. The tables below summarize the contents of each data file and provide a description of all parameters and arrays.

A note about the file name convention: Each file has a day-of-year included in the file name. This is the day corresponding to the ascending node equator crossing time (definition of orbit start time). When the equator crossing time is near midnight UT, some or all of the data in the file may occur on the day after the day in the filename.

Table 2. Variables in the CIPS RAA Level 2A geolocation file. Fill value is NaN.

Variable Name	Units	Type/Dimension	Description / Example*
AIM_Orbit_Number		Integer / 1	Integer orbit number to which all data in the file applies / 53104
Version		String / 1	Data version number / 1.00
Revision		String / 1	Data revision number / 03
Product_Creation_Time		String / 1	String containing UT time at which data file was produced / Thu Feb 9 15:51:27 2017
UT_Date	yyyymmdd	Long / 1	UT date / 20170110
UT_Time	day	Double / [Nscenes]	UT time for each element (fractional date) / range: 20170110.07241- 20170110.10574
JD_Time	Julian day	Double / [Nscenes]	UT time for each element (fractional Julian day) / range: 2457763.57241 - 2457763.60574
Orbit_Start_Time	microseconds	Double / 1	GPS start time of orbit (microseconds from 0000 UT on 6 Jan 1980) / 1.1701958e+15
Orbit_Start_Time_UT	yyyy/doy-hh:mm:ss	String / 1	Start time of orbit / 2017/010-01:05:01
Orbit_End_Time	microseconds	Double / 1	GPS end time of orbit (microseconds from 0000 UT on 6 Jan 1980) / 1.1680512e+15
Nscenes		Long / 1	# of scenes in the orbit / 15
XDim		Long / 1	Number of along-orbit-track elements in the scene data arrays / 293
YDim		Long / 1	Number of cross-orbit-track elements in the scene data arrays / 145
KM_Per_Pixel	km	Float / 1	Linear dimension of square pixel occupying area of Level 2 resolution element / 7.50
Bbox	Index	Long / [4,Nscenes]	Bounding Box of each scene: Bottom-Left and Top-Right indices of the smallest rectangle which both circumscribes a set of cells on a grid and is parallel to the grid axes / [-1317, 1, 293, 145] (scene 1)
Center_Lon	Degrees	Double / 1	Center longitude of the orbit / 127.80141
Latitude	Degrees	Float / [Xdim,Ydim,Nscenes]	Latitude of each element / [293,145,15], range: 20.428 to 41.606 (scene 1)
Longitude	Degrees	Float / [Xdim,Ydim,Nscenes]	Longitude of each element; ranges from -180 to 180 / [293,145,15], range: -135.956 to -119.739 (scene 1)
Zenith_Angle	Degrees	Float / [Xdim,Ydim,Nscenes]	Solar zenith angle (SZA) of each element. The value is specified at the altitude of the maximum contribution to the Rayleigh background. Generally around 55 km but

			increasing with increasing SZA. / [293,145,15], range: 81.360 to 97.651 (scene 1).
Orbit_Track_X_Axis		Double / 3	X axis of the orbit track ECEF coordinates used for binning grid / [-0.58685432, -0.37111988, -0.71963327]
Orbit_Track_Y_Axis		Double / 3	Y axis of the orbit track ECEF coordinates used for binning grid / [0.48878327, 0.54618836, -0.68027140]
Orbit_Track_Z_Axis		Double / 3	Z axis of the orbit track ECEF coordinates used for binning grid / [0.64551756, -0.75096492, -0.13913581]
Orbit_Track_Epoch	microseconds	Double / 1	GPS time at which the orbit track axis approximately matches the true orbit track (microseconds from 0000 UT on 6 Jan 1980) / 1.1680491e+15
Data_Product		String	Description of data product in this file / 'Rayleigh Albedo Anomaly Level 2A (scenes)'
Notes		String	Any additional notes. / Blank.

* Examples are from cips_raa_2a_orbit_53104_2017-010_v01.00_r03_cat.nc.

Table 3. Variables in the CIPS RAA level 2a albedo anomaly file. Fill value is NaN.

Variable Name	Units	Type/Dimension	Description / Example*
Rayleigh_Albedo_Anomaly	Percent	Double / [Xdim,Ydim,Nscenes]	Albedo Anomaly / [293,145,15], range: -9.334 to 4.082 (scene 2)
Rayleigh_Albedo_Anomaly_Unc	Percent	Double / [Xdim,Ydim,Nscenes]	Uncertainty in Albedo Anomaly due to noise / [293,145,15], range: 0.313 to 1.853 (scene 2)
Rayleigh_Albedo	10^{-6} sr^{-1}	Double / [Xdim,Ydim,Nscenes]	Total observed albedo / [293,145,15], range: 56.957 to 287.049 (scene 2)
Overlap_Offset	Percent	Double / [4,Nscenes]	Camera normalization factor added to RAA for each image / [4,15], [0.2192, -0.5246, 0.6391, -0.3338] (scene 2)
Overlap_Error	Percent	Double / [5,Nscenes]	Residual median camera differences after overlap offset / [5,15], [0.29, -0.29, 0.345, 0.049, -0.049] (scene 2)
Overlap_Error0	Percent	Double / [5,Nscenes]	Residual median camera differences before overlap offset / [5,15], [0.716, -0.849, -0.628, 1.213, 0.142] (scene 2)

* Examples are from cips_raa_2a_orbit_53104_2017-010_v01.00_r03_alb.nc.

Table 4. Variables in the CIPS RAA level 2a measurement geometry file. Fill value is NaN.

Variable Name	Units	Type/Dimension	Description / Example*
View_Angle	Degrees	Double / [Xdim,Ydim,Nscenes]	Satellite view angle / [293,145,15], range: XXX to YYY (scene 1)
Scattering_Angle	Degrees	Double / [Xdim,Ydim,Nscenes]	Solar scattering angle / [293,145,15], range: XXX to YYY (scene 1)
View_Angle_Derivative	Degrees/km	Double / [Xdim,Ydim,Nscenes]	Derivative of view angle with altitude along line of sight / [293,145,15], range: -0.028 to 8.83e-05 (scene 1)
Zenith_Angle_Derivative	Degrees/km	Double / [Xdim,Ydim,Nscenes]	Derivative of zenith angle with altitude along line of sight / [293,145,15], range: -0.0232 to 0.0224 (scene 1)

* Examples are from cips_raa_2a_orbit_53104_2017-010_v01.00_r03_ang.nc.

Table 5. Variables in the CIPS RAA level 2b geolocation file. Fill value is NaN.

Variable Name	Units	Type/Dimension	Description / Example*
AIM_Orbit_Number		Integer / 1	Integer orbit number to which all data in the file applies / 53104
Version		String / 1	Data version number / 1.00
Revision		String / 1	Data revision number / 03
Product_Creation_Time		String / 1	String containing UT time at which data file was produced / Thu Feb 9 15:51:36 2017
UT_Date	yyyyddd	Long / 1	UT date / 20170110
UT_Time	yyyymmdd.xx	Double / [Xdim,Ydim]	UT time for each pixel (fractional day) / [3600,320], range: 20170110.07241 - 20170110.10574
JD_Time	Days from epoch	Double / [Xdim,Ydim]	JD time for each pixel (fractional Julian day) / [3600,320], range: 2457763.57241 - 2457763.60574
Orbit_Start_Time	microseconds	Double / 1	GPS start time of orbit (microseconds from 0000 UT on 6 Jan 1980) / 1.1680455e+15
Orbit_Start_Time_UT	yyyy/doy-hh:mm:ss	String / 1	Start time of orbit / 2017/010-01:05:01
Orbit_End_Time	microseconds	Double / 1	GPS end time of orbit (microseconds from 0000 UT on 6 Jan 1980) / 1.1680512e+15
XDim		Long / 1	Number of along-orbit-track elements in the data arrays / 3600

YDim		Long / 1	Number of cross-orbit-track elements in the data arrays / 320
KM_Per_Pixel	km	Float / 1	Linear dimension of square pixel occupying area of Level 2 resolution element / 7.50
Bbox	Index	Long / [4]	Bounding Box: Bottom-Left and Top-Right indices of the smallest rectangle which both circumscribes a set of cells on a grid and is parallel to the grid axes / [-1800, -160, 3600, 320]
Center_Lon	Degrees	Double / 1	Center longitude of the orbit / 127.80141
NLayers		Integer / [Xdim,Ydim]	Number of observations at the location of each element; each observation corresponds to a different observing geometry and thus scattering angle in the phase function / [3600,320], range: 1 to 2.
Latitude	Degrees	Float / [Xdim,Ydim]	Latitude of each element / [3600, 320], range: -89.9804 to 74.8148
Longitude	Degrees	Float / [Xdim,Ydim]	Longitude of each element; ranges from -180 to 180 / [3600, 320], range: -180.0 to -180.0
Zenith_Angle	Degrees	Float / [Xdim,Ydim]	Solar zenith angle (SZA) of each element. The value is specified at the altitude of the maximum contribution to the Rayleigh background. Generally around 55 km but increasing with increasing SZA. / [3600, 320], range: 50.5209 to 99.6370
Orbit_Track_X_Axis		Double / 3	X axis of the orbit track ECEF coordinates used for binning grid / [-0.586, -0.371, -0.719]
Orbit_Track_Y_Axis		Double / 3	Y axis of the orbit track ECEF coordinates used for binning grid / [0.488, 0.546, -0.680]
Orbit_Track_Z_Axis		Double / 3	Z axis of the orbit track ECEF coordinates used for binning grid / [0.646, -0.751, -0.139]
Orbit_Track_Epoch	microseconds	Double / 1	GPS time at which the orbit track axis approximately matches the true orbit track (microseconds from 0000 UT on 6 Jan 1980) / 1.1680491e+15
Data_Product		String	Description of data product in this file / 'Rayleigh Albedo Anomaly Level 2B (scenes)'
Notes		String	Any additional notes. / Blank.

* Examples are from cips_raa_2b_orbit_53104_2017-010_v01.00_r03_cat.nc.

Table 6. Variables in the CIPS RAA level 2b albedo anomaly file. Fill value is NaN.

Variable Name	Units	Type/Dimension	Description / Example*
Rayleigh_Albedo_Anomaly	Percent	Double / [Xdim,Ydim]	Albedo Anomaly / [3600,320], range: -6498.4895 to 2686.5918
Rayleigh_Albedo_Anomaly_Unc	Percent	Double / [Xdim,Ydim]	Uncertainty in Albedo Anomaly due to noise / [3600,320], range: 0.00 to 462.239
Rayleigh_Albedo	10^{-6} sr ⁻¹	Double / [Xdim,Ydim]	Total observed albedo / [3600,320], range: -1.204 to 495.023

* Examples are from cips_raa_2b_orbit_53104_2017-010_v01.00_r03_alb.nc.

7. References

Bailey, S. M., G. E. Thomas, D. W. Rusch, A. W. Merkel, C. D. Jeppesen, J. N. Carstens, C. E. Randall, W. W. McClintock, and J. M. Russell III (2009), Phase functions of polar mesospheric cloud ice as observed by the CIPS instrument on the AIM satellite, *J. Atmos. Sol. Terr. Phys.*, 71, 373–380, doi:10.1016/j.jastp.2008.09.039.

Lumpe, J. D., S.M. Bailey, J.N. Carstens, C.E. Randall, D. Rusch, G.E. Thomas, K. Nielsen, C. Jeppesen, W.E. McClintock, A.W. Merkel, L. Riesberg, B. Templeman, G. Baumgarten, and J.M. Russell, III (2013), Retrieval of polar mesospheric cloud properties from CIPS: algorithm description, error analysis and cloud detection sensitivity, *J. Atmos. Solar-Terr. Phys.*, <http://dx.doi.org/10.1016/j.jastp.2013.06.007>.

McPeters, R. D. (1980), The behavior of ozone near the stratopause from two years of BUW observation, *J. Geophys. Res.*, 85, 4545–4550, doi:10.1029/JC085iC08p04545.

Randall, C. E., J. Carstens, J. A. France, V. L. Harvey, L. Hoffmann, S. M. Bailey, M. J. Alexander, J. D. Lumpe, J. Yue, B. Thurairajah, D. E. Siskind, Y. Zhao, M. J. Taylor, and J. M. Russell, III (2017), New AIM/CIPS global observations of gravity waves near 50-55 km, *Geophys. Res. Lett.*, 44, 7044–7052, <http://dx.doi.org/10.1002/2017GL073943>.

Created by Jerry Lumpe and Cora Randall, June 2017.